

50 years of electron biprism -50 years of exciting electron physics- *

Hannes Lichte[†]*Triebenberg Laboratory, Institute of Structure Physics,
Dresden University, D 01062 Dresden, Germany*

(Received 26 September 2003; Accepted 22 November 2003; Published 10 February 2004)

In 1953, Gottfried Moellenstedt invented the electron biprism, more or less by accident, with the serendipity characteristic to him: Aiming at dark-field imaging in an electron microscope, he stretched a thin tungsten wire across the objective aperture to block off the zero beam. However, instead of a dark field image, because of inadvertent charging of the wire under the beam, he found two images of the ZnO-needles serving as an object. Instead of trying the dark field imaging over and over again, he asked what the effect would be if the obtained two images were superimposed. Is coherence given? Moellenstedt, educated by Walther Kossel in diffraction of electron waves, had a vision: Together with his PhD-student Heinrich Dueker, he developed the electron biprism, consisting of a $1\mu\text{m}$ thin wire deliberately chargeable by means of a voltage source, as a beam splitter for coherent superposition of the electron waves passing the filament on the right and on the left. In 1955 they published the first results showing biprism interference fringes [G. Moellenstedt and H. Dueker, *Naturwiss.* **42**, 41 (1955)], which, since then, gave access to the understanding of electron waves and their use for analysis of object structures up to atomic dimensions. [DOI: 10.1380/ejssnt.2004.52]

Keywords: Electron Interference; Electron Coherence; Electron Holography

I. ELECTRON WAVES

An electron wave $\Psi_0 = \exp(i2\pi\vec{k} \cdot \vec{r})$ propagating through space with an electric potential $V(x, y, z)$ and a magnetic vector potential $\vec{A}(x, y, z)$, in a detector plane at a given z -coordinate exhibits a phase shift

$$\varphi(x, y) = \sigma V_{proj}(x, y) - 2\pi \frac{e}{h} \Phi(x, y) \quad (1)$$

with respect to field-free vacuum. $V_{proj}(x, y) = \int_z V(x, y, z) dz$ is the potential integrated along a trajectory through the point (x, y) , and $\Phi(x, y) = \oint \vec{A} \cdot d\vec{s}$ the magnetic flux enclosed by the trajectory and a reference path. Additionally, the amplitude of the wave may change due to e.g. inelastic scattering or diffraction effects; consequently, in the detector plane, the resulting wave reads as

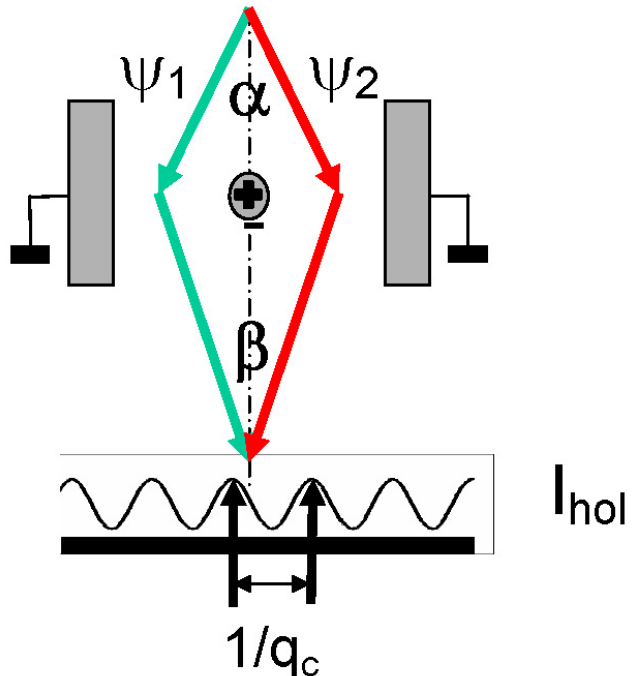
$$\Psi(x, y) = a(x, y) \exp\{i\varphi(x, y)\} \cdot \Psi_0. \quad (2)$$

with the spatial frequency

$$q_c = \frac{|\vec{k}_1| + |\vec{k}_2|}{2\beta} \quad (4)$$

of the interference fringes (Fig. 1), and

$$\mu_{12} = |\mu_{12}| \exp(i\rho_{12}), \quad (5)$$



II. SCHEME OF ELECTRON BIPRISM INTERFEROMETRY

Two correspondingly modulated waves $\Psi_1 = a_1 \exp(i\varphi_1) \exp(i2\pi\vec{k}_1 \cdot \vec{r})$ and $\Psi_2 = a_2 \exp(i\varphi_2) \exp(i2\pi\vec{k}_2 \cdot \vec{r})$ superimposed at an angle β form an interference pattern (hologram)

$$I_{hol}(x) = a_1^2 + a_2^2 + 2 |\mu_{12}| a_1 a_2 \times \cos\{2\pi q_c x + (\varphi_1 - \varphi_2) + \rho_{12}\} \quad (3)$$

*This paper was presented at The 4th International Symposium on Atomic Level Characterizations for New Materials and Devices (ALC '03), Kauai, Hawaii, USA, 5-10 October, 2003.

[†]Corresponding author: Hannes.Lichte@triebenberg.de

FIG. 1: Moellenstedt-type Electron Interferometer. Two waves $\Psi_{1,2}$, superimposed by means of the positively charged electron biprism, form a two-beam interference pattern in the detector plane, consisting of cosinoidal fringes of spatial frequency q_c . Wave properties, such as coherence and modulation in amplitude and phase, can thoroughly be analyzed from the fringe pattern.

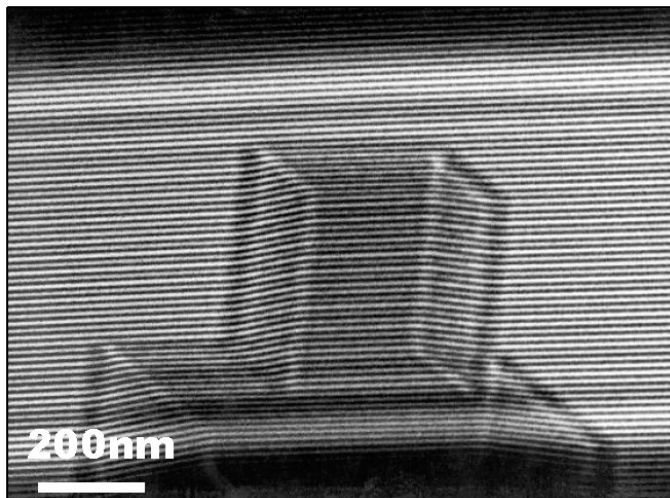


FIG. 2: Interference micrograph of a MgO-crystal. Interference fringes are damped in contrast by object amplitude and shifted laterally by object phase. Here, the phase shift stems from the mean inner potential of MgO.

the mutual degree of coherence. Furthermore, a mismatch between the amplitudes $a_{1,2}$ dampens the fringe contrast, whereas the phase difference $\Delta\varphi = \varphi_1 - \varphi_2$ induces a corresponding lateral fringe displacement (Fig. 2). In a row of experiments, Moellenstedt and coworkers investigated the basic properties of electron waves and fundamental phase shifting effects, *e.g.* the Ehrenberg-Siday-Aharonov-Bohm-Effect.

III. COHERENCE MEASUREMENTS

Electron coherence can be described in the same way as for photons from a non-LASER light source, since the degeneracy in phase space is comparably small in both cases. Measurements performed on both spatial coherence and temporal coherence were found in agreement with the corresponding results in light optics. Interestingly, spatial coherence can be interpreted in the electron particle image in that coherence is given only within the Heisenberg cone defined by the uncertainty relation. Evidently, coherence is preserved under elastic interaction, *e.g.* producing phase shifts, of the electrons with an object, such that interferograms can be recorded for measurement of object properties amplitude and phase.

However, by inelastic interaction provoking an energy difference larger than about 10^{-15} eV between the two interfering waves, their coherence is destroyed. Nevertheless, coherence may be preserved within an inelastically scattered electron wavefield of exactly the same energy transfer [2,3]. Recently, we found that the radius of spatial coherence in a Al-plasmon-scattered wave field is extended as far as 30 nm across the specimen [4]; this can be interpreted as the radius of a plasmon wave package in the object. Surprisingly, we also found a comparably high degree of coherence of electrons exciting plasmons at a distance of several 10 nm to the object (Fig. 3).

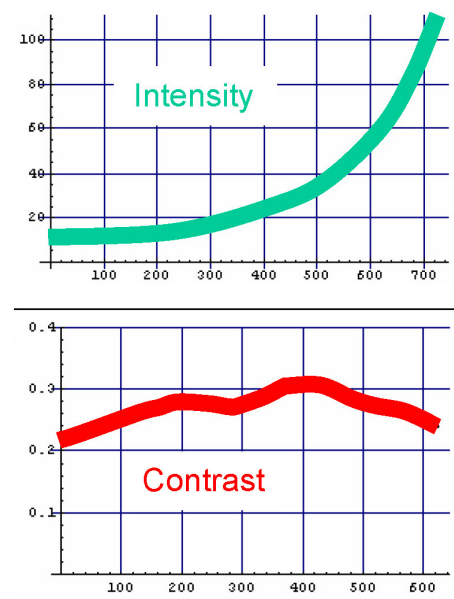
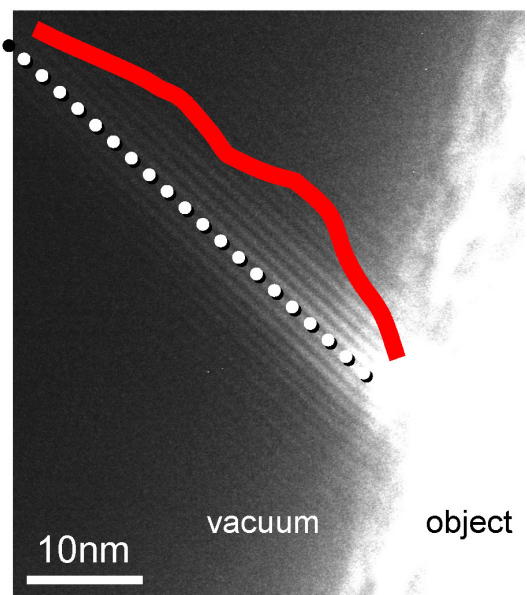


FIG. 3: Interference pattern of electrons which have excited an Al-plasmon (15.8 eV) passing by the object in vacuum. Along the dotted line, the intensity (counts per pixel) of plasmon-scattered electrons decays with distance to object, whereas the interference contrast first increases to 30% before decaying in noise.

IV. ELECTRON HOLOGRAPHY

An interferogram is a hologram, from which- by means of a reconstruction algorithm using Fourier-optics- the complex electron wave can be reconstructed both by amplitude and phase; furthermore, the reconstructed wave provides linear, zero-loss and quantitative imaging of the object structure. The specific requirements *e.g.* for fringe spacing, field of view and fringe contrast, to achieve the needed resolution and noise-properties in the reconstructed wave are outlined for example in [5], the holographic procedure is described in detail in [6].

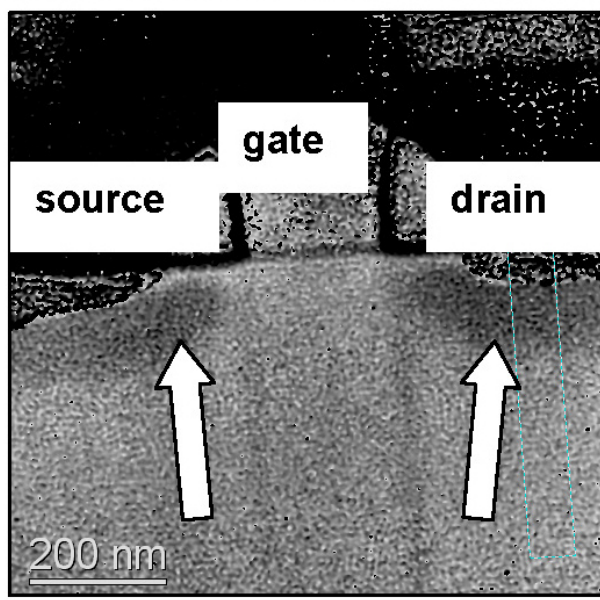
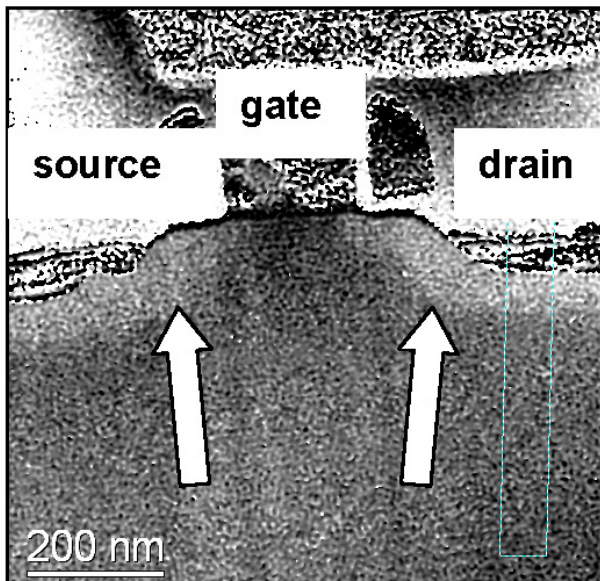


FIG. 4: Doped areas in a *n*-MOSFET (upper) and a *p*-MOSFET (lower) below source and drain, invisible in conventional electron microscopy, revealed in holographic phase images. The quantitatively measurable phase shifts arise from the potential distribution intentionally induced by the dopants, in order to control function and properties of the semiconductor device [8]. These potentials < 1 V can be measured at a lateral resolution of only a few nanometers by holography.

In particular, the availability of the phase image gives a huge advantage of holography over conventional electron microscopy. Electron holography increasingly turns out a unique tool for making use of the object information encoded in the phase. Nanoscopic electric and magnetic fields are determinable giving insight into field distributions in *e.g.* superconductors, nano-particles, doping structures of semiconductors (Fig. 4), and polarisation distribution in ferroelectrics (Figs. 5 and 6). Beautiful experiments have been reported from the Tonomura-group,

e.g. on nanomagnetics [7]. In the following, some recent results obtained in our Triebenberg-Laboratory are presented.

At atomic dimensions, the distortions stemming from aberrations of the electron microscope can be removed from the reconstructed wave by a-posteriori image processing [6]. Thereby, lateral resolution is improved by roughly a factor of 2, reaching out to 0.1 nm in both amplitude and phase; in addition, the exploitable objective aperture is opened up improving also signal/noise properties. Consequently, small differences of the phase shift from different atomic species are discernible, occurring *e.g.* between Ga ($Z=31$) and As ($Z=33$) in a GaAs-crystal (Fig. 7). This paves the way to holographic materials analysis.

V. CONCLUSIONS

After 50 years, the Moellenstedt electron biprism substantially and uniquely contributes to basic science, as well as to burning questions of solid-state physics, and even to the demands of modern nanotechnology, by answering the questions:

Where are the atoms?
Which atoms are where?
Which fields are around?

Acknowledgments

Supports from Deutsche Forschungsgemeinschaft, Koerber-Stiftung Hamburg, Volkswagen-Stiftung, and Francqui Fondation, Bruxelles are gratefully acknowledged.

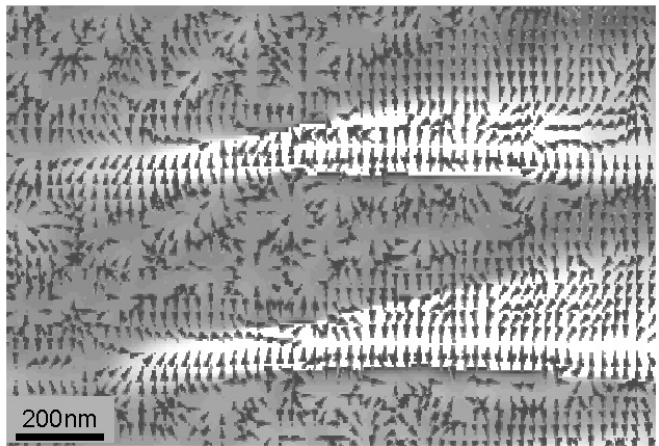


FIG. 5: Ferroelectric domains in the phase image of BaTiO₃. The arrows representing the gradient of the phase distribution indicate the in-plane polarisation of the object. In the dark domains, the randomly oriented arrows indicate no in-plane polarization. At the transition to the bright domains, the arrows align hence suggest the local polarization distribution in the bright domains [9].

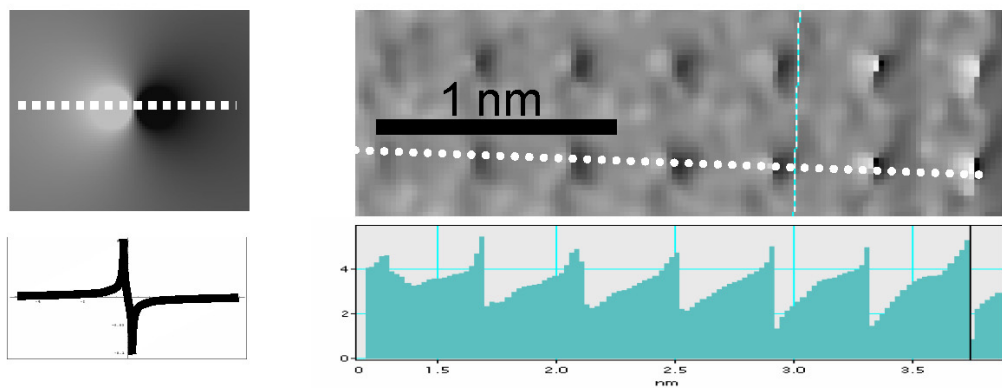


FIG. 6: Atomic dipoles in a ferroelectric crystal. Left: Simulated phase image of an electric dipole (top) with linescan (bottom). Right: Experimental phase image of (100)-oriented BaTiO₃ (top) with linescan (bottom). The thickness of the wedge shaped crystal hence the projected dipole strength increases from left to right.

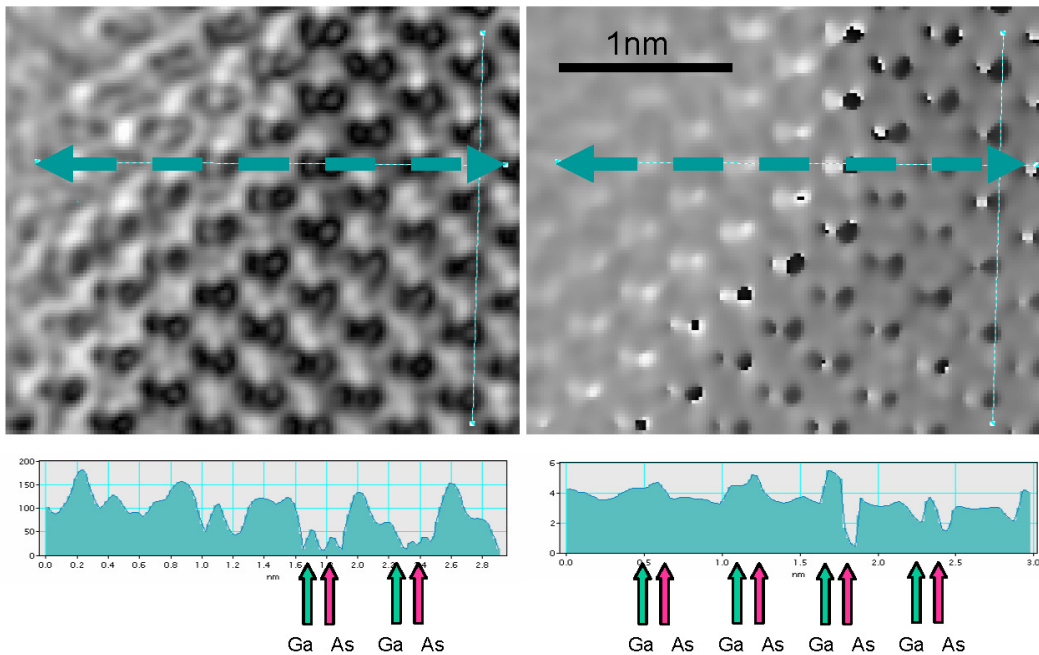


FIG. 7: Holographic materials analysis at atomic dimensions. After correction of aberrations, the dumbbell-structure of (110)-oriented GaAs shows up both in amplitude (left) and phase (right). Since the phase shift relates to the atomic number, atom species can be determined from phase shift of atomic columns. According to our experience, phases seem to be easier to interpret than amplitudes.

- [1] G. Moellenstedt and H. Dueker, *Fresnelscher Interferenzversuch mit einem Biprisma fuer Elektronenwellen*, Naturwiss. **42**, 41 (1955).
- [2] A. Harscher, H. Lichte and J. Mayer, *Interference experiments with energy filtered electrons*, Ultramicroscopy **69**, 201 (1997).
- [3] H. Lichte and B. Freitag, *Inelastic electron holography*, Ultramicroscopy **81**, 177 (2000).
- [4] H. Lichte, P. Potapov, D. van Dyck and P. Schattschneider, *Coherence in a Plasmon-Scattered Wavefield*, Microscopy and Microanalysis **9**, 84 (2003); (Proc. Microscopy Conference 2003, Dresden, Germany).
- [5] H. Lichte, *Electron interference: mystery and reality*, Phil.

- Trans. Royal Soc. Lond. **A 360**, 897 (2002).
- [6] M. Lehmann and H. Lichte, *Tutorial on Off-Axis Electron Holography*, Microscopy and Microanalysis **8**, 447 (2002).
- [7] A. Tonomura, this conference.
- [8] K. Brand, M. Lehmann, A. Lenk, H. Lichte, H.-J. Engelmann and U. Mühle, *Dopant Profiling in semiconductor devices using electron holography - influence of specimen orientation*, Proc. Int. Cong. Electron Microscopy (ICEM-15), vol.1, p.37, Durban, South Africa (2002).
- [9] H. Lichte, M. Reibold, K. Brand and M. Lehmann, *Ferroelectric Holography*, Ultramicroscopy **91**, 199 (2002).